Research on Chemical Intermediates
https://doi.org/10.1007/s11164-021-04455-1

One-pot multicomponent synthesis of *N*-sulfonyl amidines using magnetic separable nanoparticles-decorated *N*-heterocyclic carbene complex with copper

Arvind Pawar[1] · Shivanand Gajare[2] · Audumbar Patil[2] · Rajanikant Kurane[2] · Gajanan Rashinkar[2] · Suresh Patil[1]

Received: 8 November 2020 / Accepted: 29 March 2021

Abstract

Magnetic separable nanoparticles-decorated *N*-heterocyclic carbene complex with copper (MNP[1-Methyl benzimidazole]NHC@Cu) has been prepared by covalent grafting of ionic liquid like 1-methyl benzimidazole unit on the surface of chloro-functionalized Fe_3O_4 magnetic nanoparticles (MNPs) followed by metallation with copper(I) iodide. MNP[1-Methyl benzimidazole]NHC@Cu complex has been characterized by different techniques including Fourier transform infrared (FT-IR) spectroscopy, thermogravimetric analysis (TGA), energy-dispersive X-ray (EDX) analysis, X-ray diffraction (XRD), transmission electron microscopy (TEM) and vibrating sample magnetometer (VSM). MNP[1-Methyl benzimidazole]NHC@Cu complex was successfully implemented as heterogeneous catalyst in one-pot multicomponent synthesis of *N*-sulfonyl amidines from phenylacetylene, tosyl azide and amines at room temperature. Complex could be recycled six times without significant loss in the yield of product.

✉ Suresh Patil
sanyujapatil@yahoo.com

Gajanan Rashinkar
gsr_chem@unishivaji.ac.in

[1] Department of Chemistry, Padmabhushan Dr. Vasantraodada Patil College, Dist. Sangli, Tasgaon, Maharashtra 416312, India

[2] Department of Chemistry, Shivaji University, Kolhapur, Maharashtra 416004, India

Published online: 19 April 2021

Graphic abstract

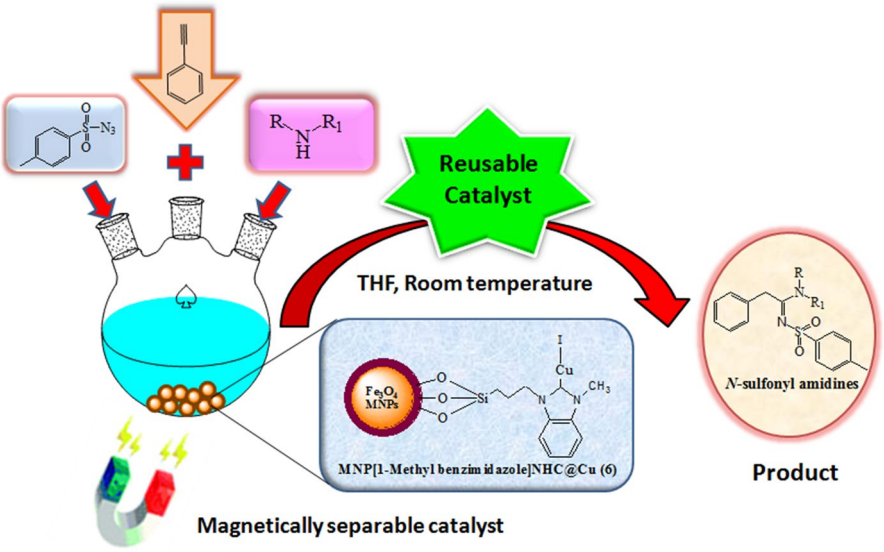

Keywords Magnetic separable nanoparticles · Multicomponent synthesis · Copper iodide · *N*-sulfonyl amidines · Reusability

Introduction

From the last ten years, *N*-heterocyclic carbenes (NHCs) have been attracted to researchers as powerful tools as ligand in organic chemistry and transition metal (TM) catalysis with numerous applications in commercially important processes [1–4]. NHCs are easily accessible, coordinative unsaturation, electron–rich, typical σ–donors and moderate π–acceptors, which sterically request structure for complexation with transition metals. A huge nature of NHC-TM structure is their unremarkable unfaltering quality that is habitually referred to as one of the fundamental advances of these ligands over their phosphine accomplices [5–9]. They are a flexible class of subordinate ligands that have gathered huge consideration for their capacity to impact different C—C, C—N and C—O bond developments in multicomponent reactions. In addition, they have remarkable properties such as high activity and selectivity with increased stability toward air and moisture, superior catalytic activities, ability to form stable metal complexes, adjustment of electronic and steric parameters, ease of access to their azolium salt precursors and tailor-made performance for specific catalytic reactions [10–12]. In spite of these properties, NHC-TM complexes have revealed the problem of contamination and recycling of catalyst during organic transformation due to their homogeneous nature [13]. To overcome these problems by replacing homogeneous

NHC-complexes with heterogeneous NHC-complexes with high area support material, this gives realm from environmental pollution and economically favorable [14]. Numbers of supporting materials have been reported with NHC-metal complexes for variety of catalytic reaction in the organic synthesis [15–17]. However, despite tremendous advances, there is considerable scope for the further development especially using magnetic nanoparticles (MNPs) as a support in order to accomplish the aim of sustainable and environmentally benign processes.

MNPs have captivated their attention in the field of catalysis due to their technology and chemical application [18, 19]. In recent years, efforts of the scientific community have been directed toward the synthesis of superparamagnetic nanoparticles for the design of magnetically retrievable nanocatalytic systems owing to their exceptional physicochemical properties and rapid response to the applied magnetic field. Among that, Fe_3O_4 MNPs are robust, inexpensive, easy to prepare, non-toxic, magnetically recoverable and can be reused multiple times for several reaction cycles. Consequently, they have emerged as the viable alternatives to existing solid-supported heterogeneous catalysts [20]. In addition, their high surface region, superparamagnetism, simple surface change by utilizing wanted functionalities and facile retrievability by external magnet have added critical adaptability for such materials in task explicit catalytic systems [21, 22]. Owing to these properties, they are widely used in synthetic chemistry [23]. Despite remarkable progress, research toward applications of Fe_3O_4 MNPs in the synthesis of magnetically retrievable NHCs is still in its infancy and therefore warrants immediate attention.

Amidines are privileged heterocyclic scaffolds with wide range of pharmacological properties such as anticancer, antimalarial, antimicrobial, antitubercular, anti-inflammatory, antioxidant, anticonvulsant and antihypertensive activities [24]. *N*-sulfonyl amidines are the important class of amidines that serve as pharmacophores, synthetic intermediates and efficient coordinating ligands [25, 26]. Owing to their extraordinary properties, a number of new advanced bespoke strategies have been developed [27–29] such as aerobic synthesis of *N*-sulfonyl amidines by using cationic copper(I) complexes from terminal alkyne, sulfonyl azide and amine [30], coupling of primary, secondary or tertiary amines and sulfonyl azides with terminal alkynes [31], chlorophosphite-mediated Beckmann ligation of oximes and *p*-toluenesulfonyl azide [32], palladium-catalyzed sulfonyl ynamide rearrangement in the presence of an amine [33], NaI-catalyzed condensation of sulfonamide and formamide [34]. Scrutiny of literature revealed that Cu-catalyzed multi-component coupling between tosyl azide, phenyl acetylene and amines represents most elegant protocol due to wide substrate scope, mild reaction conditions and potential synthetic utility. Numbers of protocols have been reported. However, there is a still scope for improvement, especially toward developing a green procedure using magnetically retrievable catalyst.

Based on aforementioned discussion and in continuation of our studies related to heterogeneous catalysis and multicomponent reaction [35–39], we report herein preparation of magnetic separable nanoparticles-decorated *N*-heterocyclic carbene complex with copper and its application in the synthesis of *N*-sulfonyl amidines.

Experimental section

General remarks

All reactions were carried out under air atmosphere in dried glassware. FT-IR spectra were measured with a Perkin-Elmer one FT-IR spectrophotometer. The samples were examined as KBr disks (~5% w/w). Raman spectroscopy was carried out using a Bruker: RFS 27 spectrometer. The thermogravimetric analysis (TGA) curves were obtained using instrument SDT Q600 V20.9 Build 20 in the presence of static air at linear heating rate of 10 °C/minute from 25 °C to 1000 °C. Elemental analyses were performed in a PerkinElmer 2400, Series II, CHNS/O analyzer and using an energy-dispersive X-ray spectroscopic facility (Hitachi S 4800, Japan). ^{1}H NMR and ^{13}C NMR spectra were recorded with a Bruker Avance (300 MHz for ^{1}H NMR and 75 MHz for ^{13}C NMR) spectrometer using $CDCl_3$ solvent and tetramethylsilane as an internal standard. Chemical shifts are expressed in parts per million (ppm), and coupling constants are expressed in hertz (Hz). Mass spectra were recorded with a Shimadzu QP2010 gas chromatography–mass spectrometry (GC–MS). The materials were analyzed by TEM using a PHILIPS CM 200 model with 20–200 kV accelerating voltages. Melting points were determined using MEL-TEMP capillary melting point apparatus and are uncorrected. X-ray powder diffraction (XRD) was taken using a Bruker D2 Phaser. Magnetic measurements were performed on Lakeshore magnetometer, USA, Model 7407. Fe_3O_4 MNPs (**1**) [40], silica coated Fe_3O_4 MNPs (**2**) [41] and all other chemicals were obtained from local suppliers and used without further purification.

Preparation of 3-chloropropyl-modified MNPs (3)

A mixture of silica-coated Fe_3O_4 MNPs **(2)** (10 g) and (3-chloropropyl)triethoxysilane (20 mL, 100 mmol) in dry xylene (100 mL) was refluxed in an oil bath. After 24 h, the reaction mixture was cooled; product was isolated by magnetic separation and washed with xylene (4 × 25 mL), methanol (4 × 25 mL), deionised water (4 × 25 mL) and dried under vacuum at 50 °C for 12 h to afford 3-chloropropyl modified MNPs (**3**). FTIR (KBr, thin film): $\upsilon = 3408$, 2925, 1099, 797, 699, 633, 583 cm^{-1}.

Preparation of MNP[1-Methyl benzimidazole]Cl (5)

A mixture of **3** (10.0 g) and 1-methyl benzimidazole (**4**) (6 g, 18 mmol) in dimethylformamide (50 mL) was heated at 80 °C in an oil bath. After 72 h, the solid was separated by magnet, washed with MeOH (3 × 50 mL), CH_2Cl_2 (3 × 50 mL) and dried under vacuum at 50 °C for 24 h to afford MNP[1-Methyl benzimidazole]Cl (**5**).

IR (KBr, thin film): υ = 3428, 2925, 2860, 1654, 1642, 1457, 1387, 1093, 585 cm^{-1}. CHNS elemental analysis observed: %C 13.42, %H 0.36, % N 4.78. Loading: 0.36 mmol functional group per gram of **5**.

Preparation of MNP[1-Methyl benzimidazole]NHC@Cu (6)

A mixture of **5** (10.0 g), copper iodide (1.9 g, 10 mmol) and NaOtBu (0.096 g, 10 mmol) in THF (50 mL) was heated at 100 °C in an oil bath for 6 h. Afterward, the mixture was separated by magnet, washed with the THF (3 × 50 mL) and dried under vacuum at 50 °C for 24 h to afford MNP[1-Methyl benzimidazole]NHC@Cu (**6**).

FT-IR (KBr, thin film): υ = 3406, 2893, 2828, 1632, 1444, 1320, 1075, 586 cm^{-1}; Elemental analysis observed: %C 13.42, % O 45.51, % Fe 14.30, % Si 19.25, % N 4.78, % Cu 1.41, % I 0.97. Loading of Cu: 0.22 mmol functional group per gram of **6**.

General method for synthesis of *N*-sulfonylamidines

A mixture of phenylacetylene (1 mmol), tosyl azide (1 mmol), amine (1.2 mmol), and MNP[1-Methyl benzimidazole]NHC@Cu (**6**) (50 mg) in THF solvent (5 ml) was stirred at room temperature. After completion of the reaction as monitored by the TLC, the complex **6** was removed by magnetic separation. Evaporation of solvent in vacuuo followed by column chromatography over silica gel using petroleum ether/ethyl acetate (8:2) afforded pure products.

NMR data of synthesized compounds:

(1) N^1, N^1-Dimethyl-2-phenyl-N^2-tosylacetamidine (Table 3, product **(10a):** ^{1}H NMR ($CDCl_3$, 400 MHz): δ 7.82 (*d*, *J* = 8.4 Hz, 2H) 7.29–7.14 (*m*, 7H), 4.42 (s, 2H), 3.11 (s, 3H), 2.92 (s, 3H), 2.38 (s, 3H) ppm; ^{13}C NMR ($CDCl_3$, 100 MHz): δ 166.7, 145.6, 142.1, 141.1, 136.2, 131.8, 129.7, 128.9,127.2, 124.6, 63.5, 41.8, 21.8 ppm.

(2) N^1, N^1-Diisopropyl-2-phenyl-N^2-tosylacetamidine (Table 3, product **(10b):** ^{1}H NMR ($CDCl_3$, 300 MHz): δ 7.84 (*d*, *J* = 7.2 Hz, 2H), 7.27–7.22 (*m*, 7H), 4.42 (s, 2H), 4.03–3.99 (m, 1H), 4.46 (s, 1H), 2.40 (s, 3H), 1.40 (*d*, *J* = 6 Hz, 6H), 0.84 (*d*, *J* = 6 Hz, 6H), ppm; ^{13}C NMR (CDCl3, 75 MHz): δ 163.4, 141.6, 141.5, 134.9, 129.0, 128.8, 127.9, 126.7, 126.2, 50.4, 48.0, 38.47, 21.4, 19.8 ppm.

(3) N^1, N^1-Diethyl-2-phenyl-N^2-tosylacetamidine (Table 3, product **(10c):** ^{1}H NMR ($CDCl_3$, 300 MHz): δ 7.78 (d, J = 6.6 Hz, 2H), 7.27–7.13 (m, 7H), 4.39 (s, 2H), 3.51 (q, 2H), 3.22 (q, 2H), 2.37 (s, 3H), 1.16 (t, J = 6.9, 6.9 Hz, 3H), 0.96 (t, J = 6.9, 6.9 Hz, 3H) ppm; ^{13}C NMR ($CDCl_3$, 75 MHz): 164.5, 141.6, 141.2, 134.3, 129.0, 128.8, 127.8, 126.7, 126.2, 43.4, 43.2, 36.5, 21.4, 13.4, 11.8 ppm.

(4) N^1-Methyl-N^1-phenyl-N^2-(4-methylbenzensulfonyl)-2-phenylacetamidine (Table 3, product **(10d):** ^{1}H NMR ($CDCl_3$, 400 MHz): δ 7.88 (*d*, *J* = 8.0 Hz, 2H), 7.28–7.20 (*m*, 5H), 7.11–7.08 (*m*, 3H), 6.83–6.77 (*m*, 4H), 4.25 (s, 2H), 3.34 (s, 3H),

2.42 (s, 3H) ppm; ^{13}C NMR (CDCl3, 75 MHz): 164.4, 142.6, 142.4, 141.5, 133.7, 129.6, 129.4, 128.9, 128.3, 127.4, 126.9, 126.6, 41.6, 35.5, 21.4 ppm.

(5) N^{1},N^{1}-Triphenyl-N^{2}-tosylacetamidine (Table 3, product **(10e):** ^{1}H NMR ($CDCl_3$, 400 MHz): 8.03 (*d*, *J* = 8.4 Hz, 2H), 7.85–7.42 (*m*, 13H), 6.75 (*d*, 4H), 4.52 (s, 2H), δ 2.45 (s, 3H) ppm; ^{13}C NMR ($CDCl_3$, 100 MHz): 165.2, 142.3, 139.5, 131.9, 128.1, 128.5, 127.8, 127.4, 126.9, 126.5, 36.9, 21.6 ppm.

(6) 2-phenyl-N,N-dipropyl-N'-tosylacetamidine (Table 3, product **(10f):** ^{1}H NMR ($CDCl_3$, 300 MHz): δ 7.76 (*d*, *J* = 7.8 Hz, 2H), 7.29–7.18 (*m*, 7H), 4.45 (*s*, 2H), 3.42 (*t*, *J* = 7.5 Hz, 7.2 Hz, 2H), 3.12 (*t*, *J* = 7.8 Hz, 7.5 Hz, 2H), 2.40 (*s*, 3H), 1.65 (*t*, *J* = 7.2 Hz, 6.9 Hz, 2H), 1.42–1.26 (*m*, 2H), 0.89–0.75 (*m*, 6H) ppm; ^{13}C NMR ($CDCl_3$, 75 MHz): *δ* 164.7, 141.4, 141.2, 134.4, 128.9, 128.8, 127.9, 126.8, 126.2, 50.7, 50.5, 36.7, 21.6, 21.4, 20.0, 11.3, 11.1 ppm.

(7) *N^{1}*, N^{1}-dibutyl-2-phenyl- N^{2}-tosylacetamidine (Table 3, product **(10 g):** ^{1}H NMR ($CDCl_3$, 300 MHz): *δ* 7.78 (*d*, *J* = 8, 4, 2H), 7.29–7.15 (*m*, 7H), 4.42 (*s*, 2H), 3.43 (*t*, *J* = 8.1 Hz, 7.5, 2H), 3.11 (*t*, *J* = 8.1 Hz, 7.8, 2H), 2.44 (*s*, 3H), 1.36–1.14 (*m*, 8H), 0.91–0.80 (*m*, 6H) ppm; ^{13}C NMR ($CDCl_3$, 75 MHz): *δ* 164.6, 141.5, 141.5, 134.5, 128.9, 128.8, 127.9, 126.7, 126.2, 49.0, 48.7, 36.9, 30.4, 28.7, 21.3, 20.2, 19.9, 13.6, 13.5 ppm.

(8) N^{1}-Isopropyl-N^{2}-(4-methylbenzensulfonyl)-2-phenylacetamidine (Table 3, product **(10 h):** ^{1}H NMR ($CDCl_3$, 400 MHz): *δ* 7.83 (*d*, *J* = 10.4 Hz, 2H), 7.86–7.18 (*m*, 7H), 4.98 (*s*, 1H), 4.27 (*s*, 2H), 4.14–4.05 (*m*, 1H), 2.42 (*s*, 3H), 1.00 (*d*, *J* = 6.4 Hz, 6H) ppm; ^{13}C NMR ($CDCl_3$, 75 MHz): *δ* 165.4, 141.7, 140.7, 133.3, 129.6, 129.3, 128.2, 126.5, 42.2, 38.5, 21.4, 21.0 ppm.

(9) N^{1}-benzyl-N^{2}-(4-methylbenzenesulfonyl)-2-phenylacetamidine (Table 3, product **(10i):** ^{1}H NMR ($CDCl_3$, 300 MHz): *δ* 7.76 (*d*, *J* = 7.9 Hz, 2H), 7.55–7.31 (*m*, 10H), 7.29–7.27 (*m*, 2H), 5.43 (*t*, 1H), 4.23 (*s*, 2H), 4.17 (*d*, 2H), 2.39 (*s*, 3H) ppm; ^{13}C NMR ($CDCl_3$, 75 MHz): *δ* 165.4, 141.4, 138.8, 134.3, 131.9, 130.4, 129.8, 129.4, 128.9, 128.2, 127.5, 126.4, 43.8, 39.7, 20.6 ppm.

(10) *N^{1},N^{1}-dinonyl-2-phenyl-N^{2}-tosylacetamidine* (Table 3, product **(10j):** ^{1}H NMR ($CDCl_3$, 400 MHz): *δ* 7.78 (*d*, *J* = 8.4 Hz, 2H) 7.27–7.14 (*m*, 7H), 4.39 (*s*, 2H), 3.39 (*t*, *J* = 7.6, 8.0 Hz, 2H), 3.0 (*t*, *J* = 8.0, 8.0 Hz, 2H), 2.38 (*s*, 3H), 1.58 (*s*, 5H), 1.32–1.21 (*m*, 25H), 0.91–0.86 (*m*, 6H) ppm; ^{13}C NMR ($CDCl_3$, 75 MHz): *δ* 165.1, 141.9, 141.2, 135.8, 129.7, 129.1, 127.8, 126.5, 125.8, 50.2, 49.7, 36.2, 31.8, 30.2, 29.1, 28.7, 27.8, 26.4, 26.1, 22.7, 21.7, 13.8 ppm.

(11) (Z)-2-(4-nitrophenyl)-1-(piperidin-1-yl)-N-tosylethanimine (Table 3, product **(10 k):** ^{1}H NMR ($CDCl_3$, 400 MHz): *δ* 7.79 (*d*, *J* = 8.4 Hz, 2H) 7.26–7.15 (*m*, 6H), 4.41 (*s*, 2H), 2.9 (*t*, 4H), 1.53 (qu, 4H), 1.21 (qu, 2H), 2.38 (*s*, 3H), ppm; ^{13}C NMR ($CDCl_3$, 75 MHz): *δ* 164.0, 145.4, 143.6, 143.4, 141.1, 130.4, 130.1, 130.0, 128.2, 121.0, 130.0, 128.2, 120.0, 45.1, 37.7, 26.0, 25.6, 26.0, 24.3 ppm.

Results and discussion

The preparation of magnetic separable nanoparticles-decorated *N*-heterocyclic carbene complex with copper is outlined in Scheme 1. Initially, Fe_3O_4 MNPs (**1**) was synthesized by co-precipitations method and coated with silica layer by using

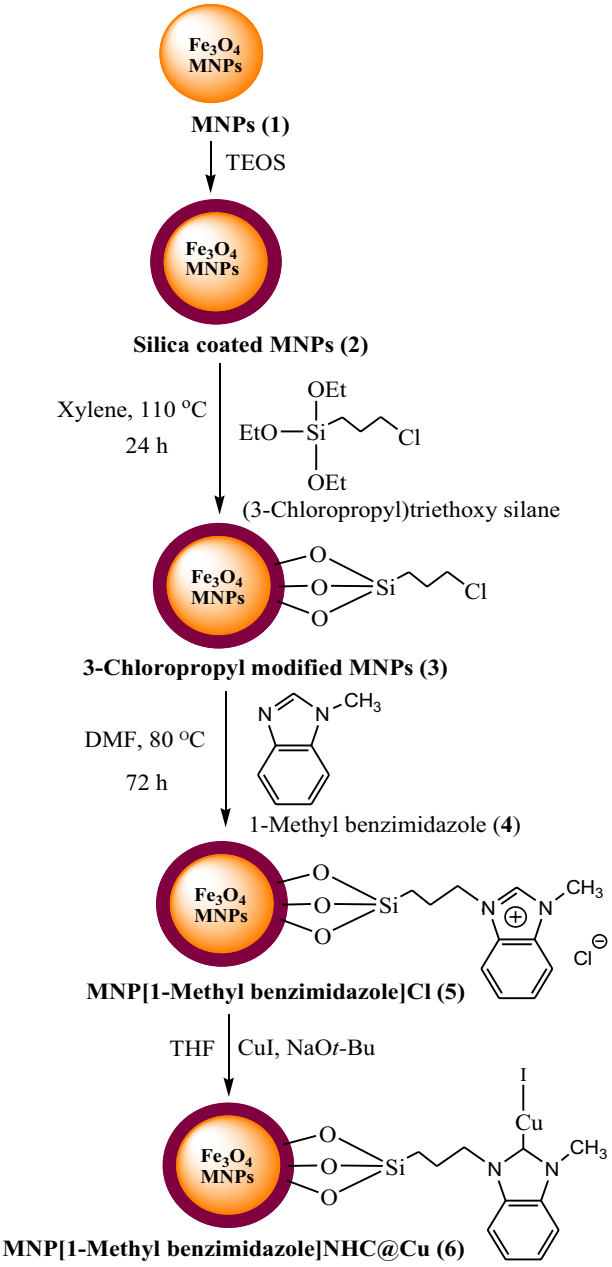

Scheme 1 Preparation of MNP[1-Methyl benzimidazole]NHC@Cu (**6**)

TEOS (tetraethyl ortho silicate) afforded silica coated MNPs (**2**) through sol–gel method [40, 41] which on further treatment with (3-chloropropyl)triethoxysilane afforded 3-chloropropyl modified MNPs (**3**). The synthetically fertile chloro group

in **3** allowed attachment of ionic liquid like group on the surface of MNPs through quaternization with 1-methyl benzimidazole (**4**) to yield azolium salt precursor acronymed as MNP[1-Methyl benzimidazole]Cl (**5**). Finally, the complexation of **5** with copper iodide by using NaOtBu as base afforded the magnetic separable nanoparticles-decorated *N*-heterocyclic carbene complex with copper acronymed as MNP[1-Methyl benzimidazole]NHC@Cu (**6**).

Fourier transform infrared (FT-IR) spectroscopy was employed to monitor reactions involved in the preparation of MNP[1-Methyl benzimidazole]NHC@Cu (**6**). The FT-IR spectrum of Fe_3O_4 MNPs (**1**) displayed Fe–O stretching band at 583 cm^{-1}. The formation of silica coated Fe_3O_4 MNPs (**2**) was confirmed by FT-IR peaks at 796, 959 and 1099 cm^{-1} attributed to Si–O–Si symmetric, Si–O symmetric and Si–O–Si asymmetric stretching modes, respectively [42]. The FT-IR spectrum of 3-chloropropyl MNPs (**3**) displayed characteristic peaks at 3408 cm^{-1} (O–H stretching), 2925 cm^{-1} (C–H stretching vibration of propyl group), 1099 cm^{-1} (Si–O stretching) (Fig. 1a) [43]. The quaternization of **3** with **4** was realized by appearance of three prominent peaks at 1654 cm^{-1} (C=N stretching vibration), 1642 cm^{-1} (C=C stretching vibration) and 1387 cm^{-1} (C–N stretching) suggesting the formation of **5** (Fig. 1b) [44]. Finally, the formation **6** was confirmed by a strong intense band of N–C–N strengthening in the range 1340–1500 cm^{-1} as a result coordination of NHC carbon ligand with copper metal ion as well as shifting of characteristic IR absorption peaks to lower frequency values (Fig. 1c) [45, 46].

The thermal stability profiles of bare Fe_3O_4 MNPs (**1**) and MNP[1-Methyl benzimidazole]NHC@Cu (**6**) were investigated by TGA analysis over the temperature range of 25–1000 ºC at a heating rate of 10 ºC/min (Fig. 2). In both cases, initial

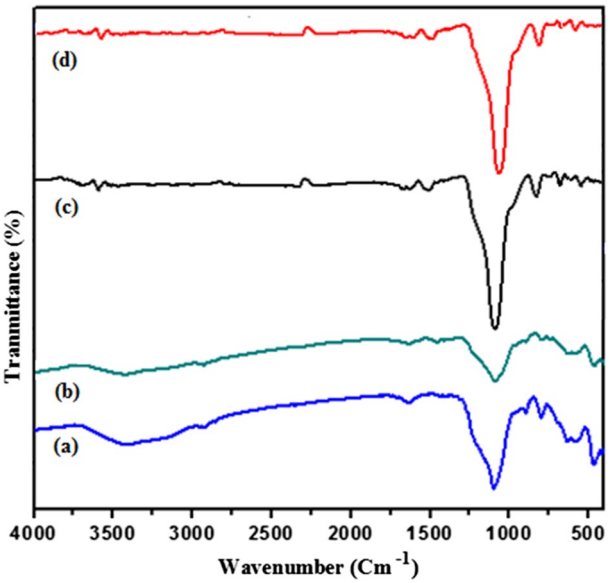

Fig. 1 FT-IR spectra of **a** 3-chloropropyl-modified MNPs (**3**); **b** MNP[1-Methyl benzimidazole]Cl (**5**); **c** MNP[1-Methyl benzimidazole]NHC@Cu (**6**); **d** reused MNP[1-Methyl benzimidazole]NHC@Cu (**6**)

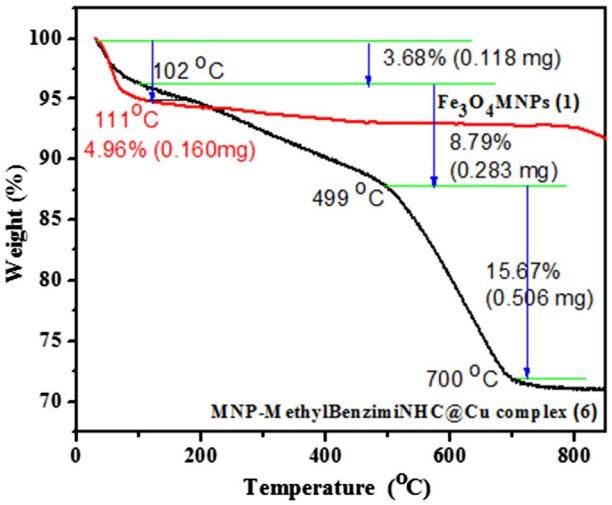

Fig. 2 TGA curves of bare Fe_3O_4 MNPs (**1**) and MNP[1-Methyl benzimidazole]NHC@Cu (**6**)

weight loss of 3.68% up to 102 ℃ and 4.96% up to 111 ℃, respectively, for **1** and **6** is due to evaporation of physically adsorbed water. TGA curve of bare Fe_3O_4 MNPs (**1**) displayed no significant weight loss from 111 to 800 ℃ which indicates that presence of only iron oxides and no any organic moiety attached on the surface of MNPs. In TGA curve of **6**, the second weight loss was observed 8.79% in the range of 102–502 ℃ attributed to loss of surface bound organic scaffolds by thermal decomposition such as (3-chrolopropyl)triethoxy silane and 1-methyl benzimidazole. The steep weight loss of 15.67% at 700 °C displayed thermal decomposition of copper iodide and major weight loss ascribed to residual silica and metallic oxides which possess high thermal stability.

The CHNS analysis of Compound [MNP-methylbenzimi]Cl (**5**) revealed that nitrogen-containing 1-methylbenzimidazole loading was 0.36 mol functional group per gram of **5**. The energy-dispersive X-ray (EDX) analysis of MNP[1-Methyl benzimidazole]NHC@Cu (**6**) displayed oxygen and iron as the major elements which are attributed to magnetic nanoparticle core of Fe_3O_4. In addition, **6** displayed minor peaks for silicon, nitrogen and iodine (Fig. 3). The presence of copper in its respective energy position also suggests the formation of complex **6**. The EDX analysis revealed loading of 0.22 mmol of Cu per gram of **6**.

The crystalline material structure and retention of Fe_3O_4MNPs in MNP[1-Methyl benzimidazole]NHC@Cu (**6**) were investigated by X-ray diffraction (XRD) analysis. The well indexing of all the peaks in diffractogram to the JCPDS card No. 86–1339 agreed retention of single-phase inverse spinel structure of Fe_3O_4 nanocore with high phase purity and crystallinity (Fig. 4). The characteristic peaks at 2θ values of 30.12°, 35.25°, 44.07°, 57.61°, 62.37°, 71.03° and 87.13° being assigned to the (2 2 0), (3 1 1), (4 0 0), (5 5 1), (4 4 0), (6 2 0) and (6 4 2) crystallographic planes of Fe_3O_4 nanocore, respectively, were observed in XRD pattern. The most intense peak is observed for (3 1 1) plane at 2θ value 35.25°. The broad peaks at 2θ from 21° to

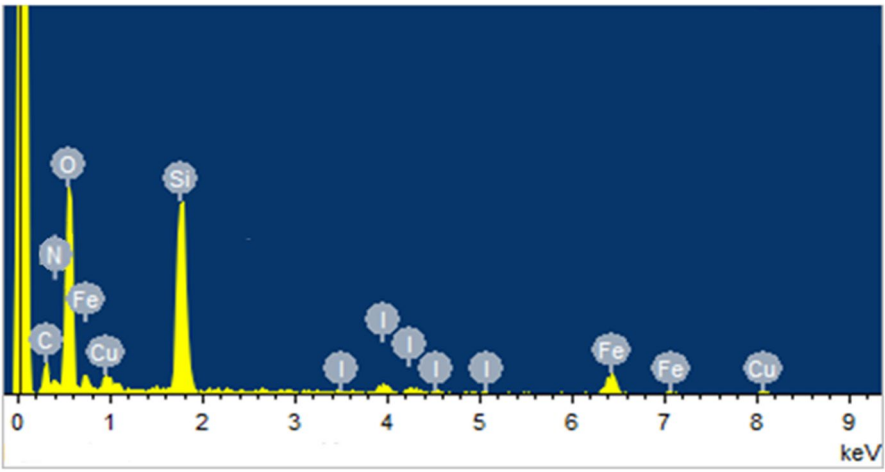

Fig. 3 EDX spectrum of MNP[1-Methyl benzimidazole]NHC@Cu (**6**)

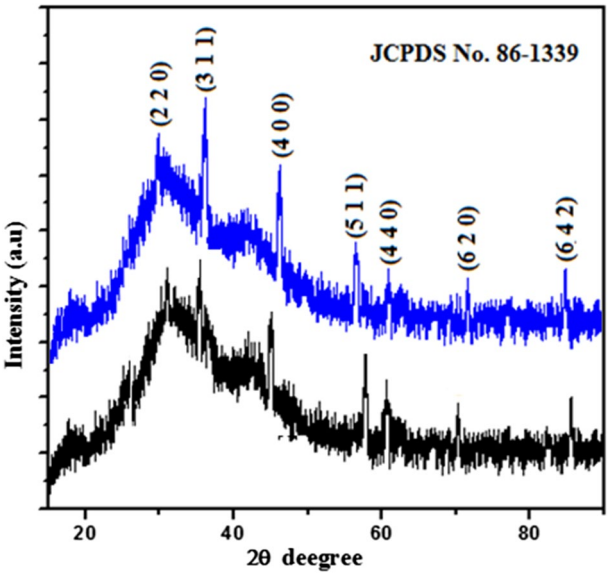

Fig. 4 XRD of MNP[1-Methyl benzimidazole]NHC@Cu (**6**) (black); XRD of reused MNP[1-Methyl benzimidazole]NHC@Cu (**6**) (blue)

32° of the XRD pattern are assigned to the silica phase. The crystallite size calculated with respect to most intense peak by using Scherrer equation was found to be 51.6 nm. The XRD analysis revealed preservation of crystallographic structure of Fe_3O_4 MNPs (**1**) in **6** even after multi-step functionalization.

The surface morphology of MNP[1-Methyl benzimidazole]NHC@Cu (**6**) was studied by transmission electron microscopy (TEM). The TEM micrographs

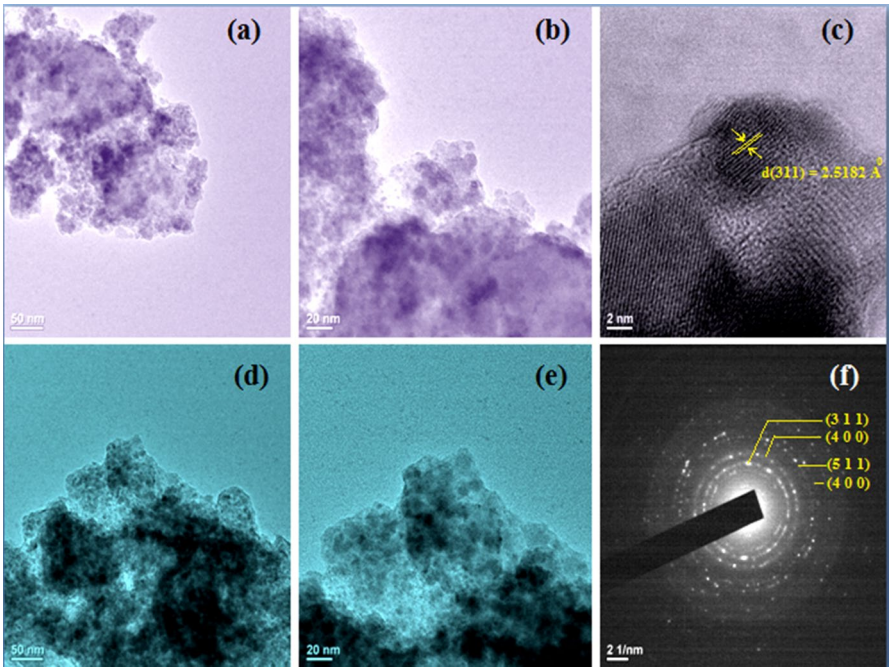

Fig. 5 TEM images of **a,b** MNP[1-Methyl benzimidazole]NHC@Cu (**6**); **c** nanoparticle shows lattice fringe width; **d-e** reused MNP[1-Methyl benzimidazole]NHC@Cu (**6**); **f** SAED pattern of MNP[1-Methyl benzimidazole]NHC@Cu (**6**)

displayed granules with spherical shape and non-smooth surface. Moreover, TEM images show embedded dark Fe_3O_4 nanocores surrounded by gray shell (Fig. 5a, b) [47]. The average nanoparticle size of 6 was found to be 10 nm with a lattice fringe width distance of $d_{(311)} = 2.5182^{\circ}$A, which reveals the formation of perfect crystal structure (Fig. 5c). The selected-area electron diffraction (SAED) pattern exhibited four strong diffraction rings which were assigned to the (3 1 1), (4 0 0), (3 3 1) and (4 2 2) bright dotted with ring pattern persuade the polycrystalline nature of Fe_3O_4 MNPs (**1**) (Fig. 5d).

The magnetic properties of bare Fe_3O_4 MNPs (**1**) and MNP[1-Methyl benzimidazole]NHC@Cu (**6**) were evaluated by magnetic hysteresis loops at room temperature using vibrating sample magnetometer (VSM) shown in Fig. 6. The saturation magnetization (Ms) values for bare Fe_3O_4 MNPs (**1**) and **6** were found to be 53 $emug^{-1}$ (Fig. 6a) and 30 $emug^{-1}$ (Fig. 6b), respectively. The saturation magnetization value of **6** exhibited comparatively low. This quenching of Ms value is ascribed due to surface functionalization [48]. However, magnetization exhibited by **6** was sufficient to enough for effective separation by external magnet.

In order to optimize the reaction conditions, a model reaction between phenyl acetylene (**7**; 1.0 mmol), tosyl azide (**8**; 1.0 mmol) and dimethylamine (**9a**; 1.2 mmol) in the presence of MNP[1-Methyl benzimidazole]NHC@Cu (**6**) was carried out at room temperature for the synthesis of *N*-sulfonyl amidines (Scheme 2).

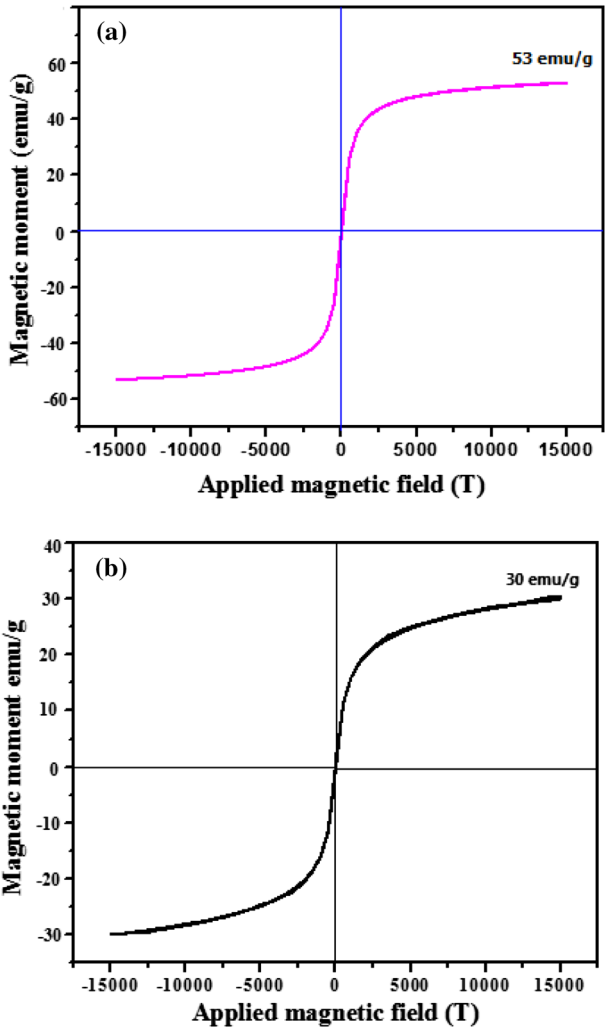

Fig. 6 **a** Magnetic curve (VSM) of bare Fe_3O_4 MNPs (**1**), **b** magnetic curve (VSM) of MNP[1-Methyl benzimidazole]NHC@Cu (**6**)

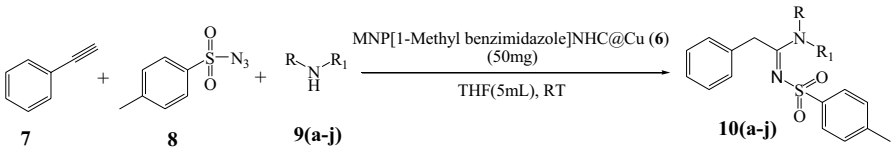

Scheme 2 MNP[1-Methyl benzimidazole]NHC@Cu (**6**) catalyzed synthesis of *N*-sulfonylamidines

Table 1 Optimization of solvent in synthesis of *N*-sulfonyl amidines [a, b]

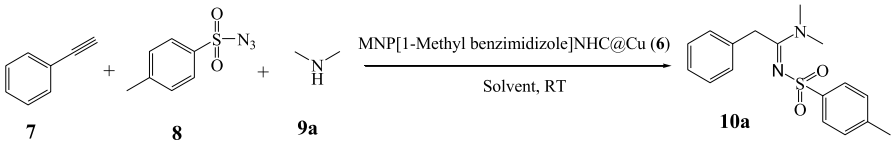

7 **8** **9a** **10a**

Entry	Solvent	Time (min)	Yield (%)	TON	TOF (h^{-1})
1	Water	2880	35	3181	66
2	DCM	260	71	6454	1490
3	**THF**	**50**	**94**	**8545**	**10,295**
4	$CHCl_3$	220	40	3636	993
5	Ethanol	240	55	5000	1250
6	Methanol	235	60	5454	1394
7	Toluene	290	45	4090	846
8	1,4-Dioxane	560	40	3636	389

Bold text indicate that it is a outstanding results compared to other entries

[a] Reaction condition:: phenyl acetylene (1.0 mmol), tosyl azide (1.0 mmol), dimethylamine (1.2 mmol), solvent (5 mL)

[b] Isolated yields after chromatography

Initially, the effect of various solvents on the model reaction was investigated in the presence of **6** at room temperature (Table 1). The reaction afforded poor yield of **10a** in water (Table 1, entry 1), whereas better yields were obtained in polar aprotic solvents such as dichloromethane (DCM), tetrahydrofuran (THF) (Table 1, entries 2–3). Further, moderate yield of **10a** was obtained in non-polar solvent such as chloroform toluene and 1–4 dioxane (Table 1, entry 4, 7 and 8). Moreover, moderate yields were achieved in polar protic solvents like methanol and ethanol (Table 1, entries 5–6). Among all the screened solvents, THF furnished the highest yield **10a** (Table 1, entry 3). Therefore, THF was chosen as the solvent for further studies.

A control reaction was carried out in which model reaction was carried out using Fe_3O_4 MNPs (**1**) and MNP[1-Methyl benzimimidazole]Cl (**5**). The reaction could not be initiated by using **1** and **5** in spite of using high quantities (up to 200 mg), indicating that they were ineffective as catalysts for the projected reaction (Table 2, entry 1–2). Next, the effect of catalyst loading was investigated on the model reaction. In the presence 10 mg (0.0022 mmol) and 20 mg (0.0044 mmol) of **6**, low amount of corresponding product, viz. N^1,N^1-Dimethyl-2-phenyl-N^2-tosylacetamidine **(10a)**, was formed even after prolonged reaction time (Table 2, entry 3–4). Gratifyingly, when the amount of catalyst was increased from 30 mg (0.0066 mmol) to 50 mg (0.011 mmol), the yield of **10a** was elevated up to 94% (Table 2, entry 5–7). However, no substantial alteration has been occurred in the yield of product and reaction time using quantities beyond 50 mg up to 200 mg (Table 2, entries 8–10). Thus, 50 mg of **6** was selected as optimal catalyst loading for further studies.

Table 2 Optimization of catalyst loading in synthesis of *N*-sulfonyl amidines [a]

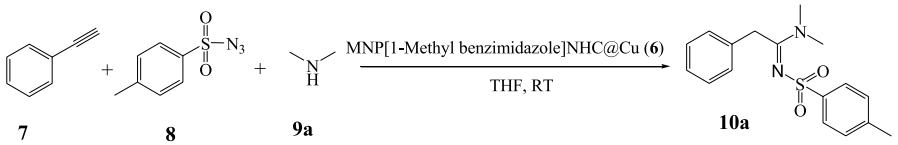

7 **8** **9a** **10a**

Entry	Catalyst	Amount of catalyst (mg)	Time (minute)	Yield[b] (%)	TON	TOF (h^{-1})
1	Fe_3O_4 MNPs (**1**)	200	2880	–	–	–
2	MNP[1-Methyl benzimidazole] Cl (**5**)	200	2880	–	–	–
3	MNP[1-Methyl benzimidazole] NHC@Cu (**6**)	10	110	48	21,818	11,992
4	**6**	20	90	73	16,390	11,060
5	**6**	30	80	89	13,484	10,138
6	**6**	40	65	91	10,340	9574
7	**6**	**50**	**50**	**94**	**8545**	**10,295**
8	**6**	100	45	94	4272	5696
9	**6**	150	40	95	2878	4361
10	**6**	200	40	95	2159	3271

Bold text indicate that it is a outstanding results compared to other entries

[a] Reaction condition: phenyl acetylene (1.0 mmol), tosyl azide (1.0 mmol), dimethylamine (1.2 mmol), THF (5 mL) at RT

[b] Isolated yields after chromatography

With the optimal reaction conditions in hands, the scope and generality of the methodology were illustrated for one-pot multicomponent reaction using phenylacetylene (**7**), tosyl azide (**8**) and variety of amines (**9**). The results are summarized in Table 3. In all the cases, reactions proceeded smoothly affording the desired *N*-sulfonyl amidines in good to excellent yields. It is worth mentioning that amines with aliphatic chain furnished better yield than aromatic amines (Table 3, entry **10a–c** and **10f–g**). Primary amines also efficiently reacted with phenylacetylene, and tosyl azide gives corresponding good yield (Table 3, entry **10 h–j**). The reactions were clean and high yielding without generation of any side product.

A plausible mechanism of *N*-sulfonyl amidines synthesis from phenyl acetylene, tosyl azide and amines using MNP[1-Methyl benzimidazole]NHC@Cu (**6**) is outlined in Scheme 3. Initially, **6** interacts with phenylacetylene (**7**) through hydrogen bonding to afford copper acetylide intermediate (**I**). Further, addition of tosyl azide (**8**) to intermediate (**I**) to forms copper triazolyl intermediate (**II**). In the next step, the formed intermediate (**II**) subsequently discharges N_2 and produces ketenimine

Table 3 MNP[1-Methyl benzimidazole]NHC@Cu (**6**) catalyzed synthesis of *N*-sulfonyl amidines [a]

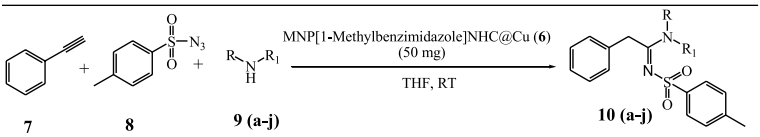

7 **8** **9 (a-j)** **10 (a–j)**

Entry	Amines (9)	Product (10)	Time (Minute)	Yield[b] (%)	TON	TOF (h^{-1})
a		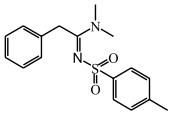	50	94	8545	10295
b		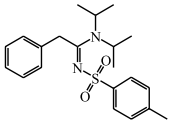	55	93	8454	9290
c		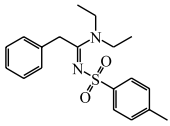	55	91	8272	9090
d		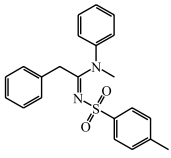	60	81	7363	7363
e	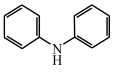	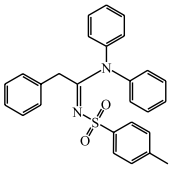	60	83	7545	7545
f	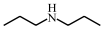	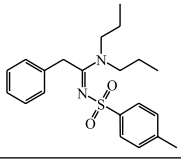	50	90	8181	9857

Table 3 (continued)

g	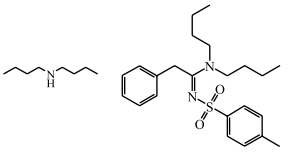	50	88	8000	9638
h	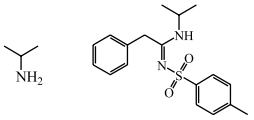	55	90	8181	8990
i	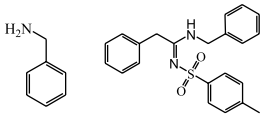	60	86	7818	7818
j	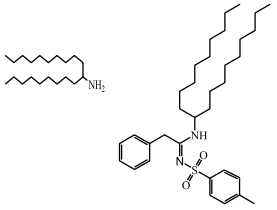	55	87	7909	8691
k	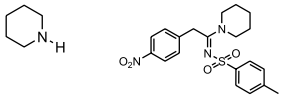	55	90	8734	9127

[a] Reaction condition: Phenyl acetylene (1.0 mmol), tosyl azide (1.0 mmol), substituted amines (1.2 mmol), solvent THF (5 mL); MNP[1-Methyl benzimidazole]NHC@Cu (**6**) (50 mg); [b] Isolated yields after chromatography

intermediate (**III**). Finally, attack of substituted amine (**9**) takes place on intermediate (**III**) which furnishes the desired *N*-sulfonyl amidines (**10a–j**) [49, 50].

To ascertain whether the reactions are truly heterogeneous, leaching studies were performed by analyzing the reaction filtrate after the recovery of MNP[1-Methyl benzimidazole]NHC@Cu (**6**) by using atomic absorption spectroscopy (AAS). Further, the hot filtration test was carried out to confirm heterogeneous nature of MNP[1-Methyl benzimidazole]NHC@Cu (**6**) by using the model reaction. In this test, a mixture of **6** (50 mg), phenylacetylene (**7a**; 1.0 mmol), tosyl azide (**8a**; 1.0 mmol) and dimethylamine (**9a**; 1.0 mmol) in THF (5 mL) was heated at 70 ºC. The **6** was separated from the hot reaction mixture when 50% conversion was accomplished (GC). The reaction was continued with the filtrate for further 6 h. There was no increase in the yield of the product beyond 50% even after 6 h confirming the heterogeneous nature of **6**.

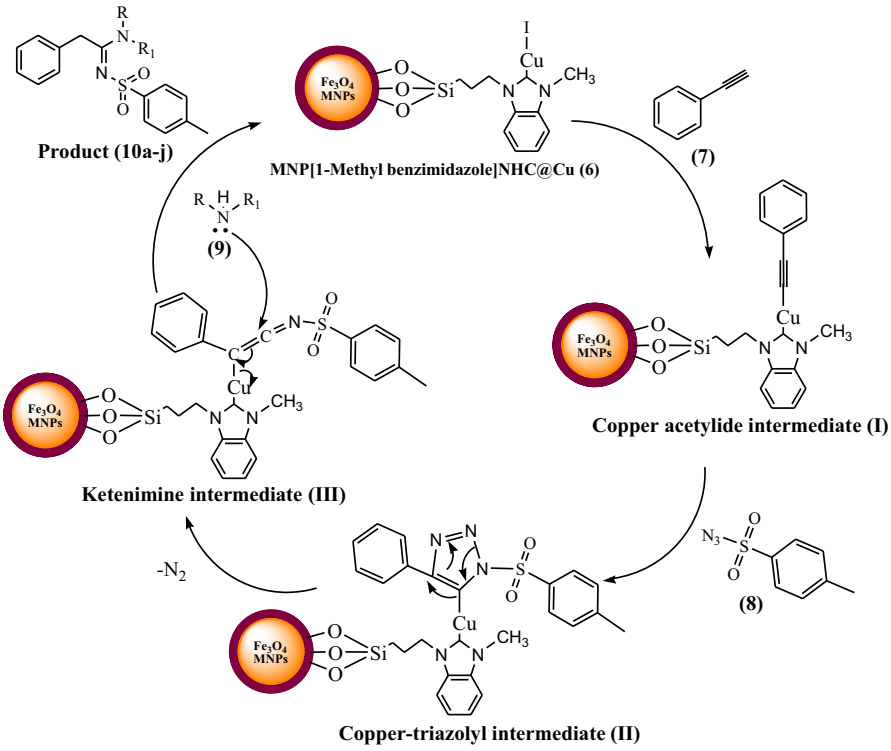

Scheme 3 A plausible mechanism for the MNP[1-Methyl benzimidazole]NHC@Cu (**6**) catalyzed synthesis of *N*-sulfonyl amidines

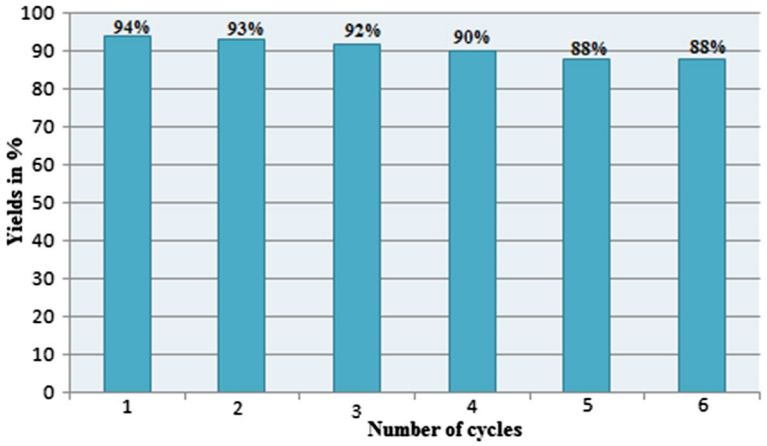

Fig. 7 Reusability of MNP[1-Methyl benzimidazole]NHC@Cu (**6**) in the synthesis of *N*-sulfonyl amidines

From the green chemistry point of view, recovery and recyclability of the supported catalyst are an unavoidable parameter for industrial and commercial scale that must be tackled for any catalytic process. Thus, the recovery and reusability of MNP[1-Methyl benzimidazole]NHC@Cu (**6**) are investigated by employing model reaction (Fig. 7). In brief, after reaction was completed, the **6** was isolated from reaction mixture by magnet. The complex **6** was washed with copious amount THF to remove organics wedded in the catalyst sites and dried under vacuum at room temperature. The amounts of necessary reactants were recalculated on the basis recovered catalyst. The recovered catalyst could be reused for six times without significant decrease in the yield of the products. Further, the stability of recycled catalyst was studied by FT-IR spectroscopy, EDX, XRD and TEM analysis of **6**. It is noteworthy to mention that the FT-IR (Fig. 1d) spectrum of reused **6** still retains the prominent peak pattern of the **6**. The EDX mapping of **6** after six catalytic cycles confirmed the integrity of the recycled catalyst. Moreover, TEM analysis of fresh (Fig. 5 a–c) and reused **6** (Fig. 5 d–e) designates that morphology is preserved even after six successive runs. The results of FT-IR, EDX, XRD and TEM analysis of fresh and reused **6** confirmed that the structural rigidity and main characteristics of complex remain conserved, demonstrating stability of **6** after six consecutive runs.

To demonstrate the importance of MNP[1-Methyl benzimidazole]NHC@Cu (**6**) in comparison with other reported methods, we have summarized previous report for synthesis of *N*-sulfonyl amidines in Table 4. The comparison of results clearly persuades that **6** is a superior catalyst in terms of catalyst loading and reaction time as compared to the reported catalyst.

Table 4 Comparison of different catalyst for synthesis of **10b**

Sr.No	Catalyst	Quantity	Solvent	Temperature	Time (min)	Yield (%)	Reference
1	$[Cu(Triaz)_2]BF_4$	1 mol%	Solvent free	RT	270	96	[30]
2	$Cu(OTf)_2$	5 mol%	Toluene	70 °C	1800	98	[49]
3	Cu-Scolecite	4.17 mol%	THF	RT	80	89	[50]
4	CuI	10 mol%	THF	25 °C	720	89	[51]
5	CuI	10 mol%	THF	RT	120	90	[52]
6	$MOF-Cu_2I_2(BTTP_4)$	2.4 mol%	THF	RT	120	89	[53]
7	CuI	10 mol%	THF	RT	120	82	[54]
8	CuI	10 mol%	THF	RT	720	89	[55]
9	Cu @C	5 mol%	CH_3CN	25 °C	180	93	[56]
10	**Present work** MNP[1-Methyl benzimidazole]NHC@Cu (**6**)	50 mg	**THF**	**RT**	**55**	**93**	**–**

Bold text indicate that it is a outstanding results compared to other entries

Conclusion

In conclusion, we have reported a magnetic separable nanoparticles-decorated *N*-heterocyclic carbene complex with copper acronymed as MNP[1-Methyl benzimidazole]NHC@Cu (**6**). The catalyst **6** was thoroughly characterized by FT-IR spectroscopy, XRD, TEM, TGA, EDX, CHNS and VSM analysis. MNP[1-Methyl benzimidazole]NHC@Cu (**6**) was successfully employed as a heterogeneous catalyst with outstanding activity in multicomponent reaction of phenylacetylene, tosyl azide and variety of amines for the synthesis of *N*-sulfonyl amidines. The protocol offers several striking advantages such as good yields, simple work up procedure, short reaction time, magnetically separable and efficient recyclability of the catalyst.

Supplementary Information The online version contains supplementary material available at https://doi.org/10.1007/s11164-021-04455-1.

Acknowledgements We gratefully acknowledge Indian Institute of Bombay (IITB), North-Estern Hill University Shillong (NEHU), Indian Institute of Technology, Madras (IITM), for providing spectral facilities and Central Facility Centre (CFC) Shivaji University Kolhapur for providing quantitative spectral analysis.

Declaration

Conflict of interest The authors declare no conflict of interest.

References

1. S.C. Sau, P.K. Hota, S.K. Mandal, M. Soleilhavoup, G. Bertrand, Chem. Soc. Rev. **49**, 1233 (2020)
2. D.M. Flanigan, F. Romanov-Michailidis, N.A. White, T. Rovis, Chem. Rev. **115**, 9307 (2015)
3. J. Cao, M. Yu, L. Hanzhu Li, X. Wang, G. Zhu, Y. Wang, C. Cao. Shi, Res. Chem. Intermed. **41**, 5323 (2015)
4. H. Diaz-Velazquez, F. Verpoort, Chem. Soc. Rev. **41**, 7032e (2012)
5. W.A. Herrmann, Angew. Chem. Int. Ed. **41**, 1290 (2002)
6. M.N. Hopkinson, C. Richter, M. Schedler, F. Glorius, Nature **510**, 485 (2014)
7. D. Janssen-Muller, C. Schlepphorst, F. Glorius, Chem Soc Rev. **46**, 4845 (2017)
8. S. Diez-Gonzalez, S.P. Nolan, Coord. Chem. Rev. **251**, 874 (2007)
9. H.V. Huynh, Chem. Rev. **118**, 9457 (2018)
10. W.J. Sommer, M. Weck, Coord. Chem. Rev. **251**, 860 (2007)
11. H.J. Huang, W.C. Lee, G.P.A. Yap, T.G. Ong, J. Organomet. Chem. **761**, 64 (2014)
12. R. Dorta, E.D. Stevens, N.M. Scott, C. Costabile, L. Cavallo, C.D. Hoff, S.P. Nolan, J. Am. Chem. Soc. **127**(8), 2485 (2005)
13. G. Guisado-Barrios, J. Bouffard, B. Donnadieu, G. Bertrand, Angew. Chem. Int. Ed. Engl. **49**, 4759 (2010)
14. C.S.J. Cazin, C. R. Chim. **12**, 1173 (2009)
15. R. Zhong, A.C. Lindhorst, F.J. Groche, F. Kuhn, Chem. Rev. **117**, 1970 (2017)
16. S. Gajare, A. Patil, S. Hangirgekar, S. Dhanmane, G. Rashinkar, Res. Chem. Intermed. **46**, 2417 (2020)
17. M. Jagadale, S. Khanapure, R. Salunkhe, M. Rajmane, G. Rashinkar, Appl. Organomet. Chem. **30**, 125 (2016)
18. A.R. Hajipour, N.S. Tadayoni, Z. Khorsandi, Appl. Organomet. Chem. **30**, 590 (2016)
19. R.B. Nasir Baig, R.S. Varma, Chem. Commun. **49**, 752 (2013)
20. R.K. Sharma, S. Dutta, S. Sharma, R. Zboril, R.S. Varma, M.B. Gawande, Green Chem. **18**, 3184 (2016)

21. P. Wang, A.G. Kong, W.J. Wang, H.Y. Zhu, Y.K. Shan, Catal Lett. **135**, 159 (2010)
22. J. Yuan, Y. Xu, A.H.E. Muller, Chem Soc Rev. **40**, 640 (2011)
23. M.B. Gawande, P.S. Branco, R.S. Varma, Chem Soc Rev. **42**, 3371 (2013)
24. M.Y. Lee, M.H. Kim, J. Kim, S.H. Kim, B.T. Kim, I.H. Jeong, S. Chang, S.H. Kim, S.-Y. Chang, Bioorg. Med. Chem. Lett. **20**, 541 (2010)
25. P. Sienkiewich, K. Bielawski, A. Bielawska, J. Palka, Environ. Toxicol. Pharmacol. **20**, 118 (2005)
26. J. Barker, M. Kilner, Coord. Chem. Rev. **133**, 219 (1994)
27. Z. Xixi, L. Yunyun, W. Jie-Ping, Chin. J. Org. Chem. **40**, 1891 (2020)
28. Z. Xixi, W. Jie-Ping, Adv. Synth. Catal. **361**, 5690 (2019)
29. D. Mishra, A.J. Borah, P. Phukan, D. Hazarika, P. Phukan, Chem. Commun. **56**, 8408 (2020)
30. F. Lazreg, M. Vasseur, A.M.Z. Slawin, C.S.J. Cazin, Beilstein J. Org. Chem. **16**, 482 (2020)
31. X. He, Y. Shang, J. Hu, K. Ju, W. Jiang, S. Wang, Sci. China Chem. **55**, 214 (2012)
32. L.M. Fleury, E.E. Wilson, M. Vogt, T.J. Fan, A.G. Oliver, B.L. Ashfeld, Angew. Chem. Int. Ed. **52**, 11589 (2013)
33. K.A. Dekorver, W.L. Johnson, Y. Zhang, R.P. Hsung, H. Dai, J. Deng, A.G. Lohse, Y.S. Zhang, J. Org. Chem. **76**, 5092 (2011)
34. S. Chen, Y. Xu, X. Wan, Org. Lett. **13**, 6152 (2011)
35. R. Kurane, J. Jadhav, S. Khanapure, R. Salunkhe, G. Rashinkar, Green Chem. **15**, 1849 (2013)
36. S. Khanapure, M. Jagadale, R. Salunkhe, G. Rashinkar, Res. Chem. Intermed. **42**, 2075 (2016)
37. S. Patil, P.B. Pawar, S.D. Jadhav, M.B. Deshmukh, Asian J. Chem. **25**, 9442 (2013)
38. S. Patil, S.D. Jadhav, M.B. Deshmukh, Arch. Appl. Sci. Res. **3**, 203 (2011)
39. A. Patil, A. Mane, S. Kamat, T. Lohar, R. Salunkhe, Res. Chem. Intermed. **45**, 3441 (2019)
40. X. Zhao, Y. Shi, T. Wang, Y. Cai, G. Jiang, J. Chomatogr A. **1188**, 140 (2008)
41. Q. Liu, Z. Xu, J.A. Finch, R. Egerton. Chem Mater. **10**, 3936 (1998)
42. M. Kooti, M. Afshari, Mater Res Bull. **47**, 3473 (2012)
43. M.A. Zolfigol, R. Ayazi-Nasrabadi, RSC Adv. **6**, 69595 (2016)
44. A. Salamatmanesh, M.K. Miraki, E. Yazdani, A. Heydari, Catal. Lett. **148**, 3257 (2018)
45. M. Pellei, V. Gandin, C. Marzano, M. Marinelli, F.D. Bello, C. Santini, Appl. Organomet. Chem. **32**, e4185 (2018)
46. M.K. Miraki, M. Arefi, A. Salamatmanesh, E. Yazdani, A. Heydari, Cat. Lett. **148**, 3378 (2018)
47. A. Ying, H. Hou, S. Liu, G. Chen, J. Yang, S. Xu, A.C.S. Sustain, Chem. Eng. **4**, 625 (2016)
48. S. Ghosh, A.Z.M. Badruddoza, M.S. Uddin, K. Hidajat, J Colloid Interface Sci. **354**, 483 (2011)
49. J. Kim, S.S. Stahl, J. Org. Chem. **80**, 2448 (2015)
50. M. Jagadale, P. Bhange, R. Salunkhe, D. Bhange, M. Rajmane, G. Rashinkar, Appl Catal A-Gen. **211**, 95 (2016)
51. S.H. Kim, S.H. Park, J.H. Choi, S. Chang, Chem. Asian J. **6**, 2618 (2011)
52. I. Bae, H. Han, S. Chang, J. Am. Chem. Soc. **27**, 2038 (2005)
53. T. Yang, H. Cui, C. Zhang, L. Zhang, C.-Y. Su, Inorg. Chem. **52**, 9053 (2013)
54. S.-J. Hwang, S.H. Cho, S.-B. Chang, Pure Appl. Chem. **80**, 873 (2008)
55. E.J. Yoo, M. Ahlquist, I. Bae, K.B. Sharpless, V.V. Fokin, S. Chang, J. Org. Chem. **73**, 5520 (2008)
56. M.J. Kim, B.R. Kim, C.Y. Lee, J. Kim, Tetrahedron Lett. **57**, 4070 (2016)